Effects of Skull Characteristics on Transcranial Focused Ultrasound Ablation

Undergraduate Honors Thesis

Presented in Partial Fulfillment of the Requirements for Honors Research Distinction in Neuroscience in the College of Engineering of The Ohio State University

By

Dylan Wyatt Beam

Food, Agricultural, and Biological Engineering

The Ohio State University

2019

Thesis Committee

Dr. Vibhor Krishna, Advisor

Dr. Ann D. Christy, Co-Advisor

Abstract

Transcranial focused ultrasound (FUS) thermal ablation is an emerging incision-less treatment for neurological disorders such as Parkinson's Disease and Essential Tremor. As an emerging treatment option, the factors affecting FUS treatment efficiency are not yet well understood. The two primary goals of this study were as follows: to investigate the relationship between skull parameters and treatment efficiency, and to create a technique to estimate temperature rise during FUS using methods and principles from statistics, heat transfer, thermodynamics, and wave mechanics.

We used a new open-source software, Kranion, to simulate FUS treatments using head Computer Tomography (CT) images. Results of simulations from 28 subjects were compared to clinical data to validate Kranion. A penetration metric (Beam Index) was calculated by combining the energy loss due to incident angles and the skull thickness.

We observed significant differences in the distribution of incident angles between different stereotactic targets in the brain. Using the Beam Index as a predictor of temperature rise, in a linear-mixed-effects model, we were able to predict the average temperature rise at the focal point during ablation with <21% error (55±3.8°C) in 75% of sonications, and with <44% (55±7.9°C) in 97% of sonications. This research suggests that the Beam Index can be used to better predict temperature rise during FUS.

Acknowledgments

This work could not have been done without the guidance of Dr. Vibhor Krishna and Dr. Francesco Sammartino. Financial support for this work was provided by the Second-year Transformation Experience Program at The Ohio State University and the Global Scholars program at the Focused Ultrasound Foundation. Results presented here were previously published by the Journal of Neurosurgery in the article titled “Kranion, an open-source environment for planning transcranial focused ultrasound surgery: technical note”. This article was authored by Dylan Beam, Dr. Francesco Sammartino, Dr. John Snell, and Dr. Vibhor Krishna.

Table of Contents

List of Tables

List of Figures

Section 1. Introduction

The first documented use of focused ultrasound (FUS) to lesion the deep brain was by the Fry brothers[4] in 1954. While this work proved the utility of FUS to create lesions in the deep brain with minimal disturbance to the surrounding tissue, this procedure still required the removal of the skull bone between the ultrasound transducer and the target to be effective. The necessity of a partial craniotomy to prevent overheating of the bone and dura mater[2], together with the realization of less invasive procedures such as gamma knife and deep brain stimulation therapy (DBS)[5] shifted the focus within the field of neurosurgery away from FUS. The work of O'Donnell and Flax in 1988[6] using phase-corrected multi-transducer ultrasound arrays, ultimately suggesting the possibility of lesioning in the brain without a craniotomy, revitalized interest in the utility of FUS for neurosurgical lesioning in the deep brain. Unilateral FUS thalamotomy to treat refractory essential tremor (ET) has recently been approved by the FDA[1] and transcranial FUS to treat Parkinson's Disease (PD) is under investigation in a phase-3 trial.

Despite technological improvements allowing FUS thermal ablation without removal of the skull, the skull is still a major barrier to the effective delivery of ultrasound energy to the brain. Currently Skull Density Ratio (SDR) is the only skull metric used in clinical practice to screen patients for FUS treatments[10]. Patients with an

SDR $\geq$ 0.4 can be treated with FUS while patients with an SDR < 0.4 are not. SDR uses CT images of a patient's skull to measure the median heterogeneity of the skull density across the effective skull area typically included in FUS treatments. However, ultrasound transmission through the skull is complex, and energy loss of a planar wave, such as an ultrasound wave, is primarily attributed to reflection of the wave at material interfaces and attenuation as the wave propagates through a medium. Therefore, we devised a novel penetration metric, the Beam Index, by modeling the path of travel of ultrasound through the skull accounting for energy loss at the water-skull interface, the energy attenuation of the wave as it travels through each layer of the skull, and the energy loss at the skull-brain interface. Combined with an understanding of the first law of thermodynamics and a basic understanding of heat transfer, the Beam Index was used to create a statistical model to predict the temperature rise during FUS ablation

Our four illustrative cases show the variability in surgical outcomes between patients with different Beam Indexes and stereotactic targets despite having similar SDR values. We then further investigated the cases of 28 subjects using imaging and treatment data to study factors associated with treatment efficiency. While it is understood that blood perfusion affects bioheat transfer, and thus the heating pattern of the deep brain tissue during FUS, and that much of the energy of ultrasonic waves is lost due to the skull, the factors affecting FUS efficiency are not fully understood. This study sought to investigate the effects of the skull on FUS treatment efficiency. This study also resulted in the characterization of the variation in the distribution of the incident angles of ultrasound beams between four deep brain targets commonly used in functional

neurosurgery. Much of this analysis was completed using a new open-source software: Kranion (https://github.com/jws2f/Kranion). Which simulates the interaction between ultrasonic waves and the skull. As it is a new software we validated Kranion by comparing the values it calculated to their clinical equivalents.

Illustrative cases

The four cases outlined in this section highlight how variable FUS treatment parameters can be between different patients. Variation in treatment efficiency between targets is exemplified by Patient A (pallidal target) and Patient B (thalamic target) which share the same SDR value (0.4). To perform the pallidotomy in Patient A, 14,000 J of energy (1,100 W for 13 seconds) was required to reach a temperature of 52°C during a sonication, and we were unable to increase the target temperature above 55°C due to significant pain during sonication. To perform the thalamotomy in Patient B, 8,300 J of energy (844 W for 10 seconds) was required to reach a similar temperature of 53°C, and we performed three sonications with a temperature >55°C. The Beam Index for Patient A was 15.5 while the Beam Index for Patient B was 21.5.

Patient C and D highlight the variation in treatment efficiency despite having the same target and similar SDR. Patient C (SDR 0.42) required 5,800 J of energy (596 W for 10 seconds) and 6,800 J of energy (696 W for 10 seconds) to reach 56°C, while Patient D (SDR 0.40) required significantly more energy (19,000 J; 850 W for 24 seconds) to reach 56°C. Patient C had a Beam Index of 42.9 and Patient D had a Beam Index of 25.8.

Section 2. Methodology

Subject Selection

Head CT images from 28 subjects with a clinical diagnosis of ET or PD being screened for FUS treatment were used for this study. Twenty-two of these subjects then received unilateral focused ultrasound lesioning of the ventral-intermediate thalamus (VIM) or the globus pallidus pars interna (GPi), making up the "treatment cohort". All subjects provided informed consent before being included in this study. IRB approval was obtained for this research which was carried out in accordance with The Code of Ethics of the World Medical Association (Declaration of Helsinki), and US Code of Federal Regulations, Title 45, Part 46, Protection of Human Subjects.

Image Acquisition and Template Image Creation

Pre-operative high resolution (voxel size 0.52x0.52X1.00 mm) spiral head CT scans were acquired from all subjects using an H60 filter (n=28) and were acquired from most subjects using an H40 series filter (n = 24). Four cubical regions-of-interest corresponding to deep structures commonly targeted in functional neurosurgery (VIM, GPi, Anterior thalamic nucleus, nucleus accumbens) were created in each hemisphere of a template T1 weighted Magnetic Resonance Image (MRI) using fslmaths, a general

image calculator tool[9] using the methods outline in Sammartino et. al[8]. The template was then aligned to each subject's head CT using the Insight Segmentation and Registration Toolkit (ITK) and exported into a Digital Imaging and Communications in Medicine (DICOM) format. Further details about the template creation can be found in Appendix A.

Planning

Template T1 and the CT images from each subject were imported into Kranion. The 'Raytracer' and 'Clip' options within the 'View' tab were selected to simulate the ultrasound waves and provide a slice view into the skull respectively. The images were then rotated such that their midlines were aligned before the focal point was placed over one of the 8 targets in the template image. To accurately model a FUS treatment, the images were then rotated together to prevent the simulated ultrasound beams from crossing the frontal sinuses and the inion, when possible. Volume outside the skull in the CT images were cropped, and the true transducer geometry for the Exablate Neuro FUS device used to treat the subjects in our treatment cohort was selected using the functionality of Kranion. To best reflect the values provided in the literature[3], 2953 m/s was used as the speed of sound in cortical bone for all simulations. Text files containing the following data for each simulated beam was then exported for further analysis: beam incident angle on the skull, skull density ratio, skull thickness, and distance traveled through the skull by the ultrasound beam. This procedure was followed eight times for each patient, once for each of the four deep brain targets on each side of the brain.

Treatment Data Acquisition

Treatment data from the 22 patients of the treatment cohort was exported from the Exablate Neuro console. The following data for each 'effective' sonication (focal point temperature ≥50°C) were manually collected from the Exablate Neuro console: energy output, sonication power, number of active elements, and focal power.

Creation of Beam Index

The ratio of energy transmitted across the skull (penetration ratio) was estimated for each ultrasound beam from an "effective element". An effective element was determined as an element with an incident angle < 20°. Elements that were active but had incident angles ≥ 20° had an estimated penetration ratio of zero. The penetration ratio was calculated by combining (multiplying) the ratio of energy transmitted across the interface between water and the skull, the ratio of energy transmitted across each layer of the skull (outer table, diploe, inner table), and the ratio of energy transmitted across the interface between the skull and the brain.

The ratio of energy transmitted across the water-skull interface and the skull-brain interface was calculated using the general equation for relative energy transmission of a planar wave across an interface:

$$T_e = 1 - \left(\frac{\rho_1 c_1 \cos\theta - \rho c \cos\theta_1}{\rho_1 c_1 \cos\theta + \rho c \cos\theta_1}\right)^2$$

Equation 1: Transmission Coefficient[12]

Where T_e is the transmission coefficient (unitless; the ratio of energy transmitted across the interface), ρ is the density (kg/m^3) of the material on the first side of the interface, c is the speed of sound (m/s) in the medium on the first side of the interface, and Θ is the incident angle (degrees) of the wave at the interface. ρ_1 is then the density of the material on the second side of the interface, c_1 is the speed of sound in the medium on the second side of the interface, and Θ is the incident angle of the wave as it leaves the interface. The values used to calculate the transmission coefficient at each of these interfaces are listed in Supplementary Table 1.

Attenuation of an acoustic wave as it propagates through a medium can be calculated using the equation:

$$A = A_0 e^{-\alpha z}$$

Equation 2: Amplitude Attenuation[11]

Where A is the amplitude of the wave after traveling through the media, z is the distance traveled by the wave through the media (m), α is the attenuation coefficient (m^{-1}) of the media, and A_0 is the amplitude of the wave as it enters the media. The ratio of the output amplitude to the input amplitude can then be expressed as:

$$A/A_0 = e^{-\alpha z}$$

Equation 3: Amplitude Ratio

Energy of a wave is proportional to the square of the amplitude of a wave, expressed as:

$$E \propto A^2$$

Equation 4: Energy and Amplitude

Therefore, a proportional change in the amplitude would result in a change of the amplitude equal to the square of that proportional change. Combining Equation 3 and Equation 4 we get:

$$E/E_0 = (e^{-\alpha z})^2$$

Equation 5: Energy Ratio

The ratio of energy transmitted through each layer of the skull (outer table, diploe, and inner table) was calculated using this equation and the values listed in Supplementary Table 1.

The mean penetration ratio of all active elements was calculated to create a raw "penetration metric". As previously stated, "effective elements" (incident angle < 20°) were calculated using the previously mentioned method while elements that were active but not effective were assigned a penetration ratio of 0. Inactive elements were not included in the calculation of the "penetration metric". To create the Beam Index, the penetration metric was linearly scaled so the minimum value of the cohort (0.0120) was equal to 1, and the maximum value of the cohort (0.1049) was equal to 100.

Temperature rise predictive model creation

A linear mixed effects model was created to predict the average temperature rise at the focal point for each sonication. Beam Index and energy delivered by the Exablate Neuro were used as covariates while the patient and their SDR were used as random effects. Temperature rise values were calculated by subtracting 37°C (average body temperature of a human) from the average peak temperature of the sonication and were

then centered by subtracting the mean temperature rise of the treatment cohort (17.26°C). The model was given the equation:

$$TemperatureRise = Energy{:}BeamIndex + (1|Patient) + (1|SDR)$$

Equation 6: Temperature Prediction Model

where "TemperatureRise" has units of °C, "BeamIndex" is unitless, and "Energy" has units of Joules. This model was created using 163 sonications from the treatment cohort of 22 patients.

Data processing and statistical analysis

Custom scripts written and implemented in MATLAB (The Mathworks, Inc.) were used for all data processing. Subjects' vendor calculated SDR and median SDR values calculated by Kranion were compared using two-sample t-tests. It was determined that the median SDR value calculated by Kranion was a more appropriate measure of center because a Kolmogorov-Smirnov test showed that the distribution of the data was not normal [$p<0.0001$]. A two-sample t-test was used to compare the following data exported from Kranion simulations: average SDR values calculated from the two different CT filters (H60 and H40 series), incident angles of transducer elements, average SDR across the different targets, and average SDR for each side of the brain. H60 filtered CT images were used for all of the analyses unless otherwise noted.

Section 3. Results

Comparison of Kranion and standard of care measurements

The Kranion calculated SDR values were not significantly different from the vendor calculated values [p=0.7895]. When comparing the number of effective elements (incident angle < 20°) estimated by Kranion to those in a treatment, no significant difference was found [Treatment=828±156, Kranion=755±103; p=0.075], however there was a significant difference when comparing the number of active elements estimated by Kranion to those in a treatment [Treatment=1001±17, Kranion=931±61; $p=5.6e^{-6}$]. Figure 1 is a visual comparison of Kranion calculated values to the clinical equivalent. Figure 1a compares the SDR values, Figure 1b compares the number of active elements, and Figure 1c compares the number of effective elements.

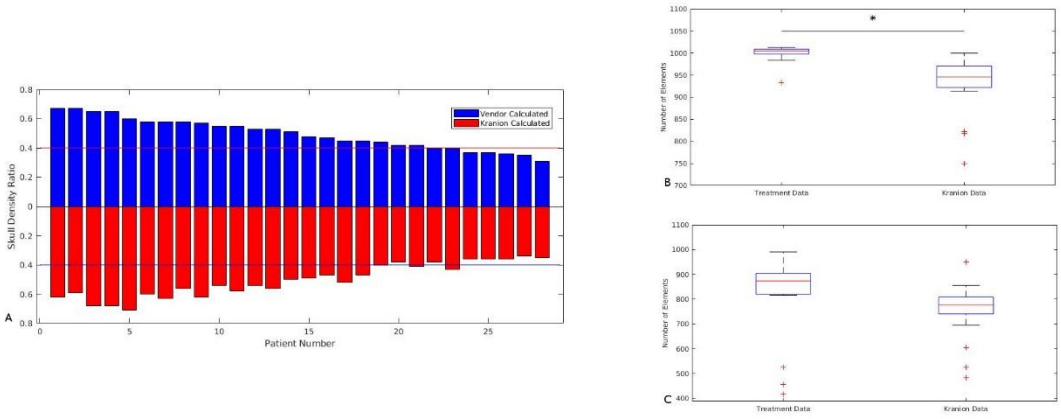

Figure 1: Comparison of Kranion to Standard of Care Measurements[8]

a) Comparative histogram of the SDR values calculated by the Vendor (blue) and SDR values calculated using Kranion (red). Lines are drawn at the SDR value of 0.4, the clinical threshold used to screen patients. 5 patients had an SDR < 0.4 with both methods, 21 patients had an SDR ≥ 0.4 with both methods, and 2 patients had an SDR ≥ 0.4 when calculated by the vendor but SDR < 0.4 when calculated with Kranion. b) Box and whisker plots comparing the number of active elements in the standard of care (left) and the value calculated by Kranion (right). There is a statistically significant difference between the two datasets. c) Box

and whisker plots comparing the number of effective elements (incident angle < 20°) in the standard of care (left) and the value calculated by Kranion (right). There is no statistically significant difference between the two datasets

Predictors of SDR

As displayed in Table 1, variance in gender, laterality of the target, or the stereotactic target had no significant effect on SDR. For the 'target' comparisons, each target was compared to the VIM dataset. A significant difference in SDR was observed when calculated using an H40 series filter versus an H60 filter (p=0.0050, 95CI [0.0312, 0.1754]).

Predictor	Category	Mean SDR ± SD	P-value	CI Lower	CI Upper
Filter	H40	0.58±0.13	0.0058	0.0315	0.1759
	H60	0.47±0.12			
Gender	Male	0.51±0.12	0.4775	-0.1254	0.0603
	Female	0.48±0.10			
Laterality	Left	0.49±0.11	0.9025	-0.0282	0.0319
	Right	0.49±0.11			
Target	Accumbens	0.49±0.11	0.7927	-0.0480	0.0367
	Anterior Nucleus	0.48±0.11	0.4548	-0.0586	0.0264
	GPi	0.49±0.12	0.8680	-0.0466	0.0394
	VIM	0.50±0.11	-	-	-

Table 1: Predictors of SDR[8]

Effective element distribution by stereotactic target

Generally, elements on the contralateral side of the target are effective more frequently. The number of effective elements in simulations of the pallidal target was significantly lower than those with the thalamic target [538±46 vs. 784±55, p<0.0001]. Figure 2 shows how frequent each element of the transducer was effective (angle < 20 degrees) across the simulations from all 28 subjects, where different colors represent how

frequently that color was considered effective during the simulations. An element that was effective all 28 simulations is dark blue, while an element that was effective for 0 simulations is yellow.

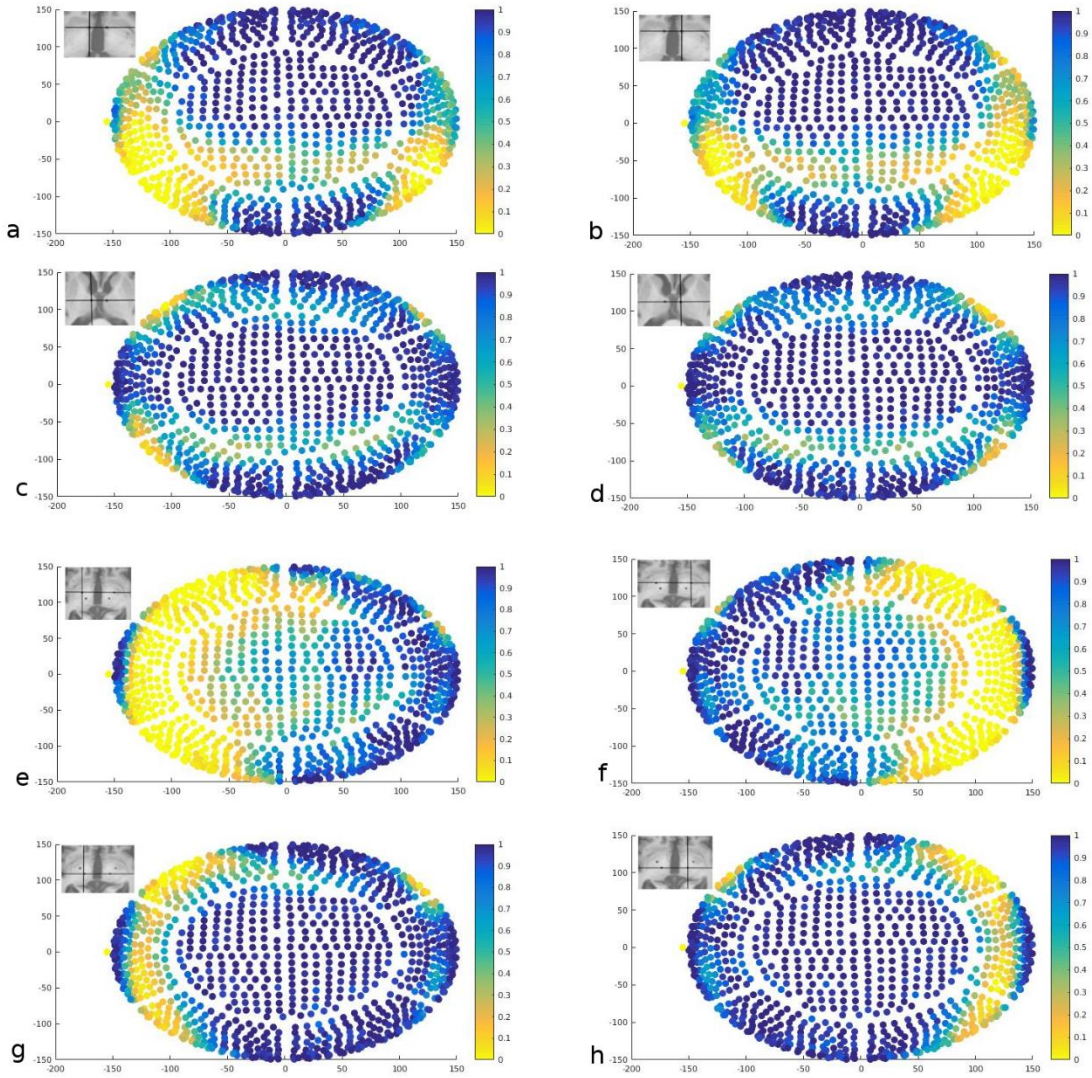

Figure 2: Effective Element Distribution for Various Targets[8]

Scatter plots where the x- and y-coordinates of a circle indicate the location of an individual transducer element on the array, and the color of each circle indicates the frequency of which the transducer element was effective (incident angle < 20°) for the indicated structure. a) left nucleus accumbens b) right nucleus accumbens c) left anterior thalamic nucleus d) right anterior thalamic nucleus e) left GPi f) right GPi g) left VIM h) right VIM

Variation of the Beam Index by stereotactic target

Table 2 displays shows how Beam Index varies between different stereotactic targets within the population of 28 subjects. Laterality had no significant effect on the Beam Index [p=0.6922]. Significant differences were found between the VIM and nucleus accumbens [40.94±21.00 vs. 30.44±18.66 p=0.0061] as well as between the VIM and GPi [40.94±21.00 vs. 29.16±15.00 p=$8.9615e^{-4}$], but no significant difference was found between the VIM and anterior nucleus [40.94±21.00 vs. 40.38±22.75 p=0.8920].

Predictor	Compared Values	Mean Metric ± SD	p-Value
Laterality	Left	34.69±19.90	0.6922
	Right	37.75±20.56	-
Target	Anterior nucleus	40.38±22.75	0.8920
	Accumbens	30.44±18.66	0.0061
	GPi	29.16±15.00	8.9615e-4
	VIM	40.94±21.00	-

Table 2: Beam Index Variation by Target[8]

Prediction of average temperature rise

The linear-mixed-effects (LME) model had a covariate coefficient of $7.37e^{-6}$, t-statistic of 6.0504, p=$9.78e^{-9}$, 161 degrees of freedom and a y-intercept of -2.5318. In 75% of sonications the LME predicted the temperature rise within 3.8°C when the measured temperature was ≤ 55°C, and in 97% of sonications the LME predicted the temperature rise within 7.9°C when the measured temperature was ≤55°C in 97% of sonications.

Section 4. Discussion

Evaluation of Skull Metrics

The differences in treatment efficiency between Patient A and Patient B paired with the common understanding that incident angle has significant effects on the efficacy of FUS provided motivation to further investigate the effect of incident angle on FUS efficiency. However, the differences in treatment efficiency between Patient C and Patient D showed that incident angle alone would likely not provide a satisfactory explanation. We found a negative correlation between skull thickness and SDR [r=-0.5817, p=0.0012] [Supplementary Figure 1] and there is an exponential, inverse relationship between the thickness of a material and the proportion of energy transmitted through the material by a planar wave[11]. This provided the additional rationale to create a skull metric accounting for factors of incident angle and skull thickness.

The behavior of the ultrasound waves as they travel through the skull is only one of the many technical challenges in FUS treatments. Energy loss of planar waves, such as ultrasound, is primarily caused by reflection and refraction at an interface between two media and by attenuation as the wave travels through a media. Bone is a porous material; meaning there are many bone-soft tissue interfaces spread throughout. Due to this nature of the bone, it is likely that the ultrasound wave would travel through many of these interfaces as it propagates from one side to the other and as such would lose energy at

each of these interfaces. As a measure of the heterogeneity of the skull, SDR seeks to capture the essence of the energy lost due to this phenomenon, however it does not account for the thickness of the skull or the incident angle of ultrasound waves on the skull. Conversely, Beam Index captures the energy loss effects of the incident angle on the skull and the thickness of the skull but assumes a certain level of homogeneity in each layer of the skull in predicting the amount of energy transmitted through the skull. Ideally, a skull metric would account for all three of these variables when predicting the amount of energy transmitted through the skull.

We displayed that the Beam Index could be used to predict temperature rise during individual FUS sonications. Since the temperature achieved in a surgery is one of the indicators of a successful surgery, we believe that Beam Index could be utilized as an additional screening tool for patients in the future to the same extent that SDR is used. Additionally, since Beam Index varies between targets (while SDR does not) and can provide temperature predictions, Beam Index may be a useful tool in screening new potential deep brain targets for investigation.

Limitations

While the Beam Index was able to predict the temperature during sonications with a certain degree of confidence, it is not yet a clinically viable tool. The Beam Index does not account for local tissue characteristics, or more nuanced principles of bioheat transfer in its temperature prediction. 2D-thermometry data was collected for this study which could provide bias and inaccuracy in the measured temperature values. While this is a

limitation of the current technologies available, improved thermometry techniques would improve the ability to investigate predictors of temperature rise. This was a retrospective which creates limitations on its own; however, this also means that all patients used for creating and validating the temperature predictive model had an SDR ≥ 0.4. Furthermore, the limited sample size and relative homogeneity of the cohort (similar ages and ethnicities) may provide additional and significant sources of bias to this study. Ideally, future studies would be done prospectively and include subjects from several centers with wider variability in age, ethnicity, and SDR.

Section 5. Conclusions

Summary

Laterality, gender, and stereotactic target do not affect SDR; however, the imaging filter used when calculating SDR may have an effect. The distribution of effective elements, as well as Beam Index, varies between different stereotactic targets. Beam Index may be useful in estimating treatment efficiency; however, estimations could be improved through use of more rigorous computational models.

Future Directions

Future techniques to estimate the amount of energy that is transmitted through the skull could be improved by accounting for bone porosity and utilizing more advanced multi-layer modeling techniques[7].

Future temperature prediction models could benefit from utilizing a more mechanistic method of relating the energy transmitted through the skull to the temperature increase. This could be done by using heat transfer equations and accounting for local tissue characteristics measured with imaging data.

Contributions

Subjects were selected for this study by Dr. Vibhor Krishna. Images were acquired by the Department of Radiology at The Ohio State University Wexner Medical Center. The template image was created by Dr. Francesco Sammartino. Planning and simulations were done by Dylan Beam under the supervision of Dr. Francesco Sammartino. Treatment data were acquired during FUS treatments that were run by Dr. Vibhor Krishna and was then collected from the console by Dylan Beam and Dr. Francesco Sammartino. The Beam Index and linear mixed-effects model were created by Dylan Beam. All other statistical analyses as well as all the figures were created by Dylan Beam.

References

1. FDA Approves Focused Ultrasound to Treat Essential Tremor. 2016, July 12. Charlottesville (VA): Focused Ultrasound Foundation; [accessed 2019, April 4]. https://www.fusfoundation.org/the-foundation/news-media/fda-approves-focused-ultrasound-to-treat-essential-tremor.
2. Fry FJ. 1977. Transkull transmission of an intense focused ultrasonic beam. Ultrasound Med Biol (3):179-184.
3. Fry F, Barger J. 1978. Acoustical properties of the human skull. The Journal of the Acoustical Society of America (63)**:**1576-1590.
4. Fry WJ, Mosberg Jr W, Barnard J, Fry F. 1954. Production of focal destructive lesions in the central nervous system with ultrasound. Journal of neurosurgery (11):471-478.
5. Heath RG. 1963. Electrical self-stimulation of the brain in man. American Journal of Psychiatry (120):571-577.
6. O'donnell M, Flax S. 1988. Phase-aberration correction using signals from point reflectors and diffuse scatterers: Measurements. IEEE transactions on ultrasonics, ferroelectrics, and frequency control (35):768-774.
7. Pichardo S, Sin VW, Hynynen K. 2010. Multi-frequency characterization of the speed of sound and attenuation coefficient for longitudinal transmission of freshly excised human skulls. Physics in Medicine & Biology (56):219.
8. Sammartino S, Beam DW, Snell J, Krishna V. 2019. Kranion, an open-source environment for planning transcranial focused ultrasound surgery: technical note. Journal of Neurosurgery.
9. Smith SM, Jenkinson M, Woolrich MW, Beckmann CF, Behrens TE, Johansen-Berg H, et al. 2004. Advances in functional and structural MR image analysis and implementation as FSL. Neuroimage (23):S208-S219.
10. Tlusty T, Vitek S, Zadicario E. 2014 December 10. Systems and methods for optimizing transskull acoustic treatment. United States patent US2016084026A1
11. Willems H GK. 1989. Ultrasonic Attenuation Measurement Using Backscattering Technique. Springer US(8).
12. Two Dimensional Waves. 2004. Cambridge (MA): Massachusetts Institute of Technology; [accessed 2019, April 4]. http://web.met.edu/1.138j/www/material/chap-3.pdf.

Appendix A: Methods Expanded

Beam Index Creation

Variable	Value
Attenuation coefficient for cortical bone	152.28 m^{-1}
Attenuation coefficient for trabecular bone	148.28 m^{-1}
Outer table thickness	1.3 mm
Inner table thickness	1.5 mm
Water density	993 kg/m^3
Inner table density	1910 kg/m^3
Diploe density	1738 kg/m^3
Outer table density	1870 kg/m^3
Brain density	1081 kg/m^3
Speed of sound in water	1520 m/s
Speed of sound in cortical bone	2953 m/s
Speed of sound in trabecular bone	2500 m/s
Speed of sound in soft tissue (used to model the speed of sound in the brain)	1540 m/s

Table 3: Table of Values for Beam Index Calculation[8]

Appendix B: Supplementary data

Relationship between SDR and skull thickness

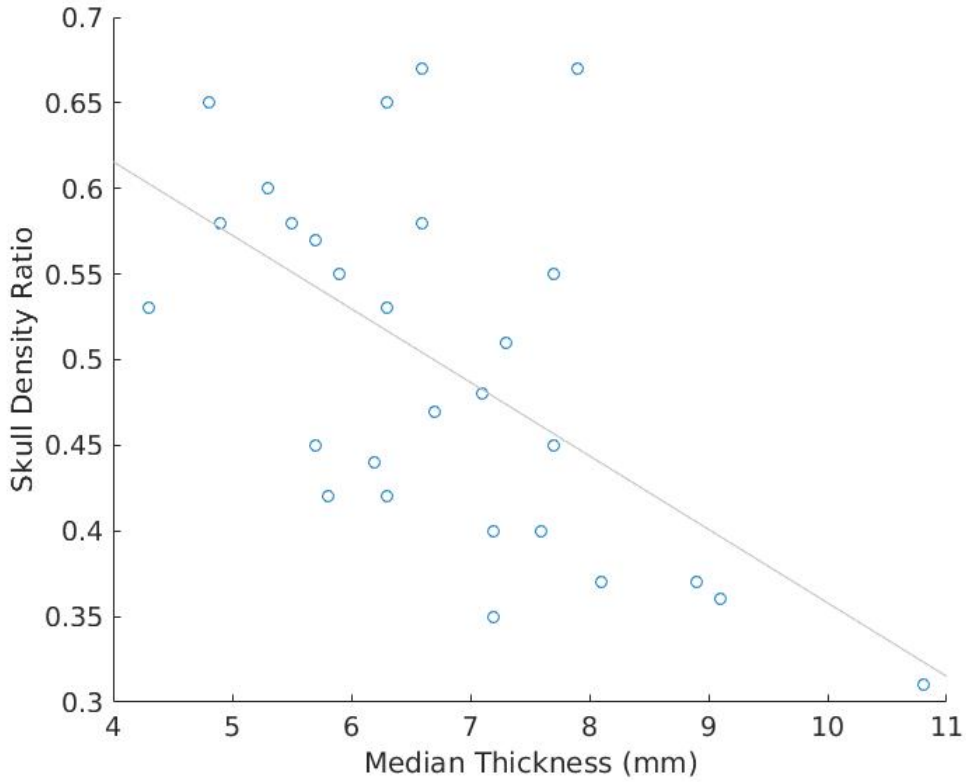

Figure 3: Average Skull Thickness vs. SDR for Each Patient[8]